Analysing limitations of the FlowCyl as a one-point viscometer test for cement paste

Rolands Cepuritis[1,2], Elisabeth L. Skare[1,3], Evgeny Ramenskiy[1,3], Ernst Mørtsell[1,5], Sverre Smeplass[1,4], Shizhao Li[3], Stefan Jacobsen[1], Jon Spangenberg[3]

[1] Department of Structural Engineering, Norwegian University of Science and Technology, NO-7491 Trondheim, Norway

[2] Norcem AS (HeidelbergCementGroup), R&D Department, Setreveien 2, Postboks 38, NO-3950 Brevik, Norway

[3] Department of Mechanical Engineering, Technical University of Denmark, 2800 Lyngby, Denmark

[4] Skanska Norge AS, Drammensveien 60, PO Box 1175, NO-0107 Oslo, Norway

[5] NorBetong AS (HeidelbergCementGroup), Heggstadmyra 6, NO-7080 Heimdal, Norway

Abstract: The FlowCyl is a simple flow viscometer – a modification of the Marsh Cone test apparatus – developed to quantify the flow behaviour of cement pastes. The FlowCyl gives a one-parameter characterisation of rheology called the flow resistance ratio or λ_Q, which is defined as the average ratio between the flow loss of a measured fluid and theoretical flow of an ideal fluid. This paper reports a study on the limitations of the FlowCyl and appurtenant flow resistance ratio. The investigation includes rheological measurements of cement pastes incorporating crushed aggregate fines with a diameter below 125 µm and development of a numerical model in order to analyse the flow condition inside the FlowCyl. The numerical simulations are carried out both with the Bingham- and Herschel-Bulkley material model of the rheometer data. A comparison with the experimental λ_Q results illustrates that only a minor error is introduced when describing the flow of cement paste in the FlowCyl with a two-parameter model (Bingham material model) as compared to a three-parameter model (Hershel-Bulkley model). The results also show that the one-parameter characterisation (*i.e.* λ_Q) mainly correlates to the plastic viscosity in the Bingham material model, while the yield stress only correlates if the dosage of superplasticizer per mass of cement is kept constant. The numerical simulations show that high shear rates at the outlet of the FlowCyl are responsible for the difference in the correlations.

Keywords: *Rheology, cement paste, FlowCyl, yield stress, plastic viscosity*

1. INTRODUCTION

As pointed out by Ferraris et. al [1], determining rheology properties by testing concrete is not always practical, easy, and economical, because execution of numerous concrete tests requires a large amount of material and manpower. Therefore, there is a need for simpler and easier laboratory approaches. It has been demonstrated that rheological measurements of cement paste can be used as a reasonable indicator of concrete rheology [1], [2], [3].

Fresh cement paste is a fluid that, just like concrete, exhibits a yield stress, requiring a minimum stress to initiate flow. Below the yield stress, cement paste behaves like a solid, which typically is a result of a three-dimensional microstructure at low stresses [4]. Above the yield stress, cement paste on the contrary deforms as a fluid according to a viscosity function that is shear rate dependent. The rheological behaviour of cement paste can be quantified by the usage of a rheometer, for example, with a parallel plate, cone and plate, coaxial cylinder, or Couette geometry [5]. The shear stress (or viscosity) as a function of shear rate and a best-fit match to the data determines the appropriate constitute law, *e.g.* the Bingham- or Herschel-Bulkley (H-B) material model [5].

As pointed out by Shaughnessy and Clark [6], measuring the rheological properties of cement paste is not a straightforward task, and substantial care must be taken prior, during and after the measurements. The most common measurement techniques, procedures and challenges were recently thoroughly reviewed by some of the authors of this paper. The review can be found in the following reference [7]. Although highly accurate rheometers are available, simple empirical test methods for rheological examination of cement paste are also quite popular, for both research and industrial purposes. This is due to relatively complex procedures of performing measurements with the rheometers, but even more importantly due to their cost. One of the most popular of the applied empirical methods include a range of mini slump-cone geometries that mainly provide the single empirical parameter, slump flow (spread diameter of the mixture), which relates to the yield stress of the cement paste [1], [8]. Another set of tests are the orifice viscometers, where the fresh cement paste flows out of different funnel-shaped containers through a narrow orifice. The mass flux or flow time is registered as the test result. Some of the most popular orifice viscometers are the Marsh cone [9], [10], mini V-funnel [1], and FlowCyl [2], [3], [11].

The FlowCyl test characterizes the rheological behaviour of cement pastes via one parameter, the flow resistance ratio (denoted λ_Q), which is described in more detail later in the paper. This test method has been successfully used to predict the workability of conventional (vibrated) normal-weight concrete mixes with consistencies of up to about 240 mm of slump, which was based on natural sand and cement paste with relatively low fines content [2]. Later, the same was shown to be possible for lightweight aggregate concrete that was based on natural sand and coarse lightweight aggregates [3]. However, in a series of further studies [11], [12], [13] it was demonstrated that the FlowCyl test result has limitations when applied to self-compacting concrete (SCC) mixes and mixes incorporating high amounts of crushed sand fines when the amount of superplasticiser was below the assumed saturation level. In the study, by Mørtsell and Smeplass [11] the hypothesis was that the proportioning model where the FlowCyl is used to characterise the viscous phase of the concrete (filler modified cement paste = matrix) would work even better with the matrix-dominated SCC mixes. Then the workability of the SCC mixes tested would be a unique function of the flow resistance ratio of the matrix determined with the FlowCyl and the volume of the matrix according to the Particle-Matrix concrete proportioning model [2]. However, the results revealed that to achieve a slump-flow measurement of approx. 650 mm, the necessary matrix volume was 40-80 l/m^3 lower for the mixes based on the high-strength ordinary Portland cement (OPC) than for the regular OPC mixes, when all other parameters (including λ_Q values) were comparable. In other words, the researchers did not find a simple correlation between the flow resistance ratio of the matrix and the workability of the SCC. Smeplass and Mørtsell [11] suggested that the problem potentially was in the measuring device used for the characterisation of the matrix, *i.e.* the FlowCyl. They theorized that the problem with the FlowCyl was that it gives only a single value, whereas the matrix is at least a two-parameter fluid and thus there is a need to get a more fundamental understanding of the limitations of this equipment.

In this paper, the objective is for the first time to analyse the limitations of the flow resistance ratio when used as a one-point parameter to describe the flow behaviour of fresh filler modified cement paste. Hereto, FlowCyl and rheometer measurements of filler modified cement pastes that cover a broad interval of flowabilities are performed and correlated. In addition, a numerical model is employed to simulate the FlowCyl tests and thereby assist in understanding/estimating the error that is introduces by going from a three-parameter (H-B material model: $\tau = \tau_0 + K\dot{\gamma}^n$, where τ_0 is H-B yield stress [Pa], K is consistency factor [Pa s^n] and n is flow index [-]) to a two-parameter (Bingham material model: $\tau = \tau_0 + \mu\dot{\gamma}$, where τ_0 is Bingham's yield stress [Pa], μ is Bingham's plastic viscosity [Pa s], while τ and $\dot{\gamma}$ are the corresponding yield stress [Pa] and shear rate [1/s]) to a one-parameter (flow resistance ratio) flow characterization of cement pastes.

2. EXPERIMENTS

2.1. Materials

Three different types of crushed aggregate fines were included in the cement pastes in order to obtain cement pastes with different rheological behaviour. All of the crushed fines originated from the same granitic rock type (typical mineralogical composition of the parent rock: feldspar 48 %, quartz 48 %, amphibolite 2 %, mica 1 %, chlorite 1 %) and were produced in the same way. The production process included four steps of rock crushing followed by a system of air-classification that was utilised to extract the generated fines from the crushed aggregates. The three types of crushed fines were extracted at different steps in the air-classification process and thus the main difference between them was their PSD. The different types of fines were denoted as **(F)-PSD**, **(C)-PSD** and **(I)-PSD**. The maximum particle size for all three types of fines was adjusted to be the same by mechanical sieving via a sieve with square opening of 125 µm edge length. The PSD of the fines, see Figure 1, was determined by a SediGraph, which is a PSD measurement tool that measures the particle sedimentation speed through x-ray absorption and calculates the equivalent particle diameter based on Stoke's law [14]. The oven-dry particle density for all of the crushed fines was determined with a helium pycnometer to be the same, *i.e.* 2.65 g/cm^3.

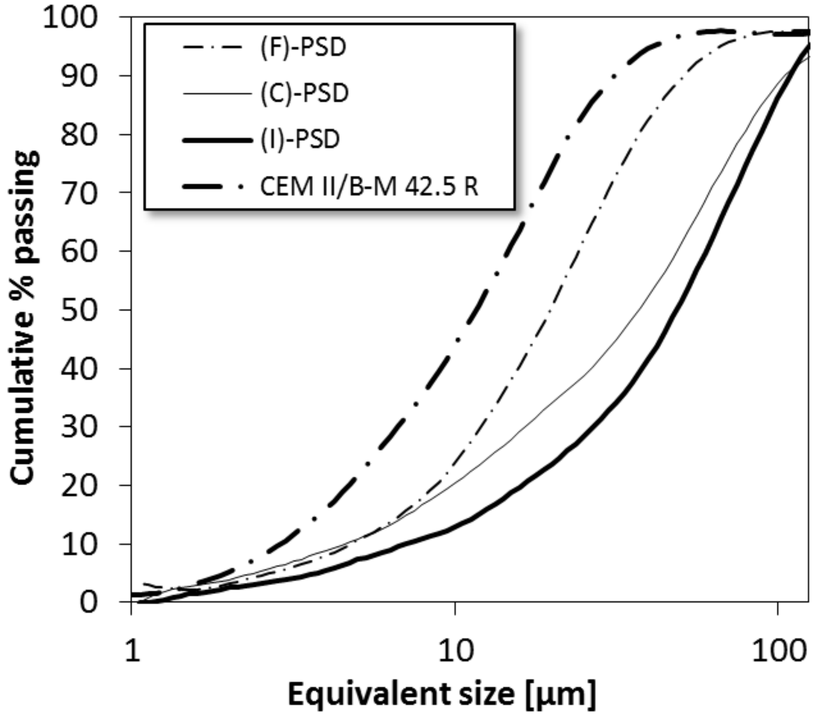

Figure 1: PSDs of the crushed aggregate fines and cement used for the experiments.

Blended cement with a particle density of 3.0 g/cm^3 incorporating 18.1 % of fly-ash and 5 % of gypsum (CEM II/B-M 42.5 R) from Norcem AS was used in all the cementitious mixes. The mineralogical composition of the clinker of the cement was C_3S: 61.0 %; C_2S: 14.2 %; C_3A: 8.8 %; C_4AF: 9.3 %; free CaO: 1.7 %; other minerals: 5.0 %. The Na_2O-eq. content of the cement was 1.3 %. The Blaine value was determined to be 422 m^2/kg and the PSD of the cement determined with the SediGraph is shown in Figure 1. Polycarboxylate ether (PCE) based superplasticiser (SP) Dynamon SR-N (solids content of 19.5 %; liquid density of 1.05 g/cm^3) from Mapei was used.

2.2. Cement paste compositions

An overview of the studied filler modified cement paste compositions is given in Table 1. The mixes were divided into “A”-series and “B-series. The “A”-series represents mixes where three different w/c ratios (0.4, 0.55 and 0.70) were combined with the three different types of crushed fines. In addition, for every w/c ratio, three different fi/c ratios were employed. The w/c and fi/c ratios were chosen with the goal of covering the range that is practically used in ready-mix concrete production with crushed sand in Norway. For the “A”-series mixes the dosage of SP was fixed at 0.75 % of the total cement mass. In the “B”-series, the SP dosage was varied for the mixes with (I)-PSD fines and w/c ratio 0.4 and 0.55 from the "A"-series, *i.e.* A10-A15. The SP dosage was increased to 1.0 %, 1.25 %, 1.5 % and 1.75 % of the total cement mass.

Table 1: Overview of the studied filled modified cement paste compositions.

Mix No.	**w/c**	**SP [%]**	**fi/c**	**PSD**	**Solid volume fraction Φ_s**	**Mix No.**	**w/c**	**SP [%]**	**fi/c**	**PSD**	**Solid volume fraction Φ_s**
A-1	0.4	0.75	0.28	(C)	0.516	**B-1**	0.40	1.00	0.28	(I)	0.516
A-2	0.4	0.75	0.36	(C)	0.531	**B-2**	0.40	1.00	0.36	(I)	0.531
A-3	0.4	0.75	0.44	(C)	0.545	**B-3**	0.40	1.00	0.44	(I)	0.545
A-4	0.55	0.75	0.51	(C)	0.477	**B-4**	0.40	1.25	0.28	(I)	0.515
A-5	0.55	0.75	0.59	(C)	0.490	**B-5**	0.40	1.25	0.36	(I)	0.530
A-6	0.55	0.75	0.67	(C)	0.502	**B-6**	0.40	1.25	0.44	(I)	0.545
A-7	0.7	0.75	0.68	(C)	0.444	**B-7**	0.40	1.50	0.28	(I)	0.515
A-8	0.7	0.75	0.76	(C)	0.456	**B-8**	0.40	1.50	0.36	(I)	0.530
A-9	0.7	0.75	0.82	(C)	0.464	**B-9**	0.40	1.50	0.44	(I)	0.544
A-10	0.4	0.75	0.28	(I)	0.516	**B-10**	0.40	1.75	0.28	(I)	0.515
A-11	0.4	0.75	0.36	(I)	0.531	**B-11**	0.40	1.75	0.36	(I)	0.530
A-12	0.4	0.75	0.44	(I)	0.545	**B-12**	0.40	1.75	0.44	(I)	0.544
A-13	0.55	0.75	0.51	(I)	0.477	**B-13**	0.55	1.00	0.51	(I)	0.477
A-14	0.55	0.75	0.59	(I)	0.490	**B-14**	0.55	1.00	0.59	(I)	0.490
A-15	0.55	0.75	0.67	(I)	0.502	**B-15**	0.55	1.00	0.67	(I)	0.502
A-16	0.7	0.75	0.68	(I)	0.444	**B-16**	0.55	1.25	0.51	(I)	0.477
A-17	0.7	0.75	0.76	(I)	0.456	**B-17**	0.55	1.25	0.59	(I)	0.490
A-18	0.7	0.75	0.82	(I)	0.464	**B-18**	0.55	1.25	0.67	(I)	0.502
A-19	0.4	0.75	0.28	(F)	0.516	**B-19**	0.55	1.50	0.51	(I)	0.477
A-20	0.4	0.75	0.36	(F)	0.531	**B-20**	0.55	1.50	0.59	(I)	0.490
A-21	0.4	0.75	0.44	(F)	0.545	**B-21**	0.55	1.50	0.67	(I)	0.502
A-22	0.55	0.75	0.51	(F)	0.477	**B-22**	0.55	1.75	0.51	(I)	0.477
A-23	0.55	0.75	0.59	(F)	0.490	**B-23**	0.55	1.75	0.59	(I)	0.489
A-24	0.55	0.75	0.67	(F)	0.502	**B-24**	0.55	1.75	0.67	(I)	0.502
A-25	0.7	0.75	0.68	(F)	0.444						
A-26	0.7	0.75	0.76	(F)	0.456						
A-27	0.7	0.75	0.82	(F)	0.464						

Abbreviations used in the table:

w/c = water-to-cement ratio by mass.
SP = superplasticiser dosage by mass of cement.
fi/c = crushed fines-to-cement ratio by volume.
PSD = particle size distribution of the crushed fines.

2.3. Methods

Mixing of the filler modified cement pastes was carried out following a routine investigated and described by Ng. et. al. [15]. This routine was chosen because, as reported by Ng. et. al. [15], it provides a level of shear rates in the fresh mix that remedy too excessive temperature rise and/ or air entrainment during the material preparation. The FlowCyl and rheometer measurements were started exactly 10 minutes after beginning the mixing procedure.

The test setup for the FlowCyl and its geometry is presented in Figure 2. The FlowCyl measurements followed the same routine as reported in [16]. During a measurement, the FlowCyl is filled with cement paste up to the level of 15 mm below the top edge, while the outlet is blocked. Then the outlet is opened and the mass of the cement paste in the bowl under the FlowCyl is registered with a sampling rate of 2 sec. Subsequently, the volumetric flow is analysed from the cement paste has a height of 35 cm in the FlowCyl until it reaches 15 cm in order to extract the flow resistance ratio (*i.e.* λ_Q), which is a dimensionless single parameter proposed by Mørtsell [2] that characterise the flowability of the cement paste. The flow resistance ratio is defined as the difference in volumetric flow rate between the tested material (fresh cement paste) and an "ideal" fluid [2] with no internal flow resistance and no external cohesion or friction, *i.e.* the flow rate for an ideal fluid is only affected by gravity (the actual expected volumetric flow rate, as function of the fluid height in the FlowCyl is provided in the references [2] and [3]). It is given by the expression:

$$\lambda_Q = F_t / F_i , \tag{1}$$

where F_t is the average difference between the theoretical flow rate of an "ideal" fluid and the measured flow rate of the tested cement paste; and F_i is the average flow rate of the "ideal" fluid. By definition, the "ideal" fluid has a λ_Q value of 0.0, while the theoretical upper limit of the λ_Q value for a viscous fluid is 1.0 [2] [2], [3]. More details on the FlowCyl and the mathematical derivation of λ_Q can be found in [2], [3], [11].

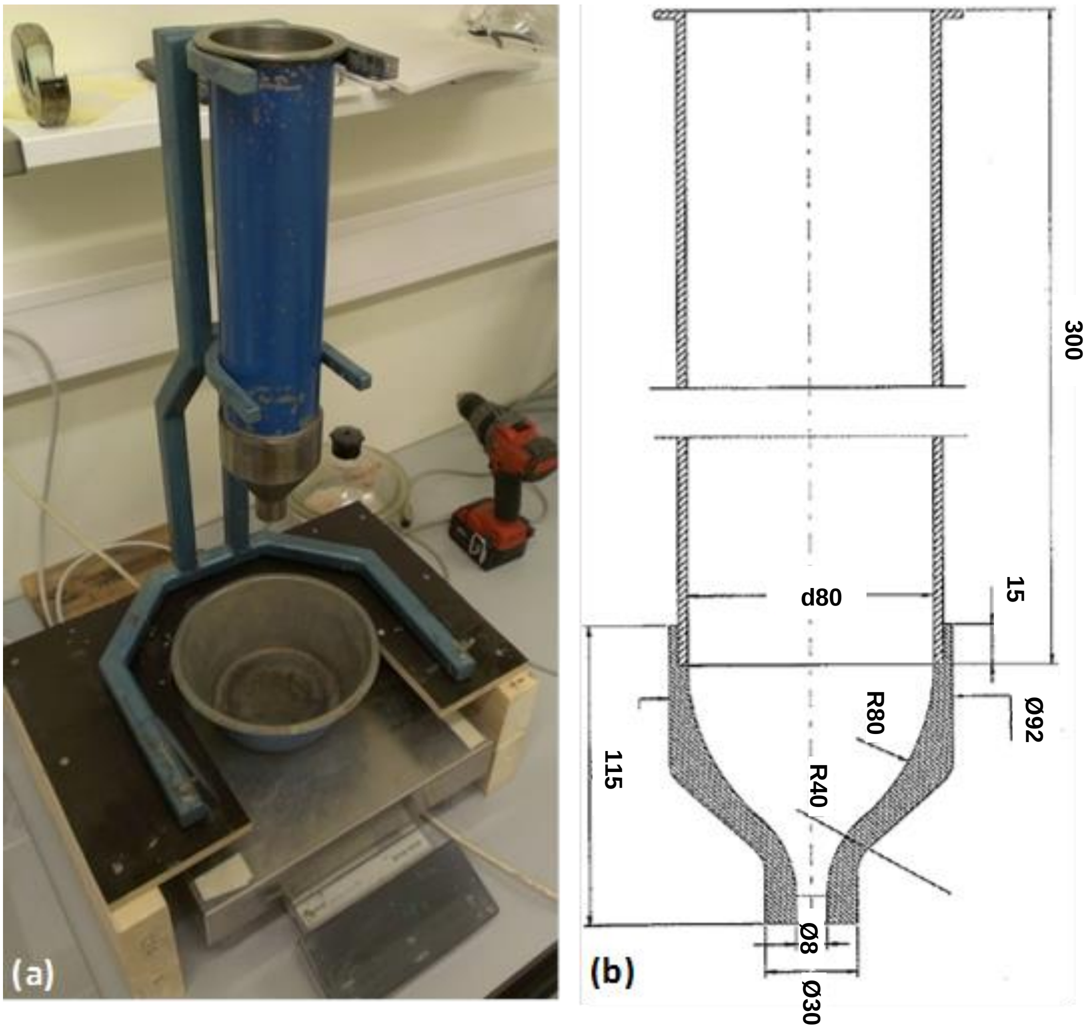

Figure 2: (a) the FlowCyl test apparatus; (b) the exact geometry of the FlowCyl test apparatus. Note that the lengths and radii are given in mm.

The rheometer measurements were done on a Physica MCR 300 rheometer (Anton Paar) with a bob-in-a-cup geometry, see Figure 3. The geometry and the used measurement routine were the same, as reported in [17]. Mathematical regression was applied on the measured down (decreasing shear rate) flow-curve data in order to obtain the Bingham and H-B material model parameters [5]. In [17], also details about the uncertainty for both the Physical MCR 300 rheometer and FlowCyl measurements can be found. It was shown in [17] that for very similar cement pastes as studied in this paper, the standard deviation for 5 repeated measurements on the same mix composition, was approximately 0.9 MPa and 0.01 Pa·s for the Bingham parameters and 0.01 units for the flow resistance ratio.

Figure 3: The bob-in-a-cup geometry used for the experiments. The surfaces of the bob have been roughened to prevent slip.

3. NUMERICAL MODEL

In the literature, numerical models have successfully been utilized to analyse different topics related to fresh cementitious materials, *e.g.* flow in reinforced formwork [18], [19], [20], gravity induced aggregate migration [21], [22], [23], [24], flow of fibers [25], [26], pumping [27], and flow conditions in rheological characterization tools [28], [29]. As mentioned in the introduction, in this study a computational fluid dynamics (CFD) model was used to analyse the flow behaviour in the FlowCyl. The CFD model was developed in the commercial software Flow3D that has been found to be very applicable for simulations of fresh cementitious materials [30]. Flow3D utilizes the finite volume method to discretize the mass- and momentum conservation equations and the generalized minimal residual method in order to solve for the pressure and velocity. The interface between the cement paste and air was tracked by the volume of fluid method [31], which is a free surface tracking algorithm that in an Eulerian frame is considered very accurate [32]. In Figure 4, the model version of the FlowCyl at time zero is illustrated. The inner surface of the FlowCyl was modelled with a wall boundary condition (zero-velocity/no-slip) and the numerically predicted flow resistance ratio was calculated in a similar way as for the experiments, except that the flow rate was determined based on the remaining volume in the simulated domain. A preliminary validation of the CFD model was presented in [13] where it was shown that the simulations predicted the flow resistance ratio within 10 % accuracy for five different cement pastes, when assuming that the cement pastes could be described by the Bingham material model. In this study, both the Bingham- and H-B material model [33] were used to describe the flow behaviour of all 52 cement pastes in order to compare their performance.

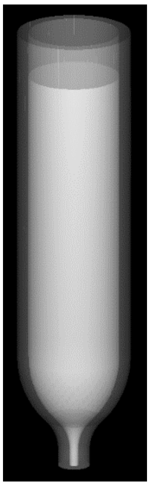

Figure 4: The model version of the FlowCyl at time zero [37].

4. RESULTS AND DISCUSSION

In Table 2, the rheological parameters for the Bingham- and H-B material model are presented for all 52 cement pastes together with the experimental- and two numerical flow resistance ratios.

Table 2: Experimental and numerical results.

Mix No.	Flow resistance ratio λ_Q			Bingham model parameters		Herschel–Bulkley model parameters			Mix No.	Flow resistance ratio λ_Q			Bingham model parameters		Herschel–Bulkley model parameters		
	M	F-3D (B)	F-3D (HB)	τ_0 [Pa]	μ [Pas]	τ_{HB} [Pa]	c [Pas^p]	p [Pa]		M	F-3D (B)	F-3D (HB)	τ_0 [Pa]	μ [Pas]	τ_{HB} [Pa]	c [Pas^p]	p [Pa]
A-1	0.890	0.866	0.887	9.36	1.09	9.39	1.09	1.00	**B-1**	0.810	0.822	0.810	7.11	0.72	6.99	0.74	0.99
A-2	0.920	0.891	0.906	14.27	1.26	14.40	1.12	1.01	**B-2**	0.849	0.869	0.849	8.32	0.97	8.59	0.92	1.01
A-3	0.960	0.920	0.929	23.98	1.40	20.67	2.25	0.89	**B-3**	0.873	0.894	0.873	11.34	1.12	11.16	1.16	0.99
A-4	0.580	0.628	0.605	2.72	0.26	2.23	0.37	0.91	**B-4**	0.780	0.798	0.780	4.15	0.62	4.71	0.51	1.05
A-5	0.590	0.678	0.647	5.02	0.31	3.40	0.76	0.80	**B-5**	0.792	0.814	0.792	4.42	0.68	5.53	0.47	1.09
A-6	0.650	0.713	0.693	4.85	0.38	3.77	0.65	0.88	**B-6**	0.814	0.826	0.814	4.59	0.80	5.13	0.69	1.03
A-7	0.390	0.481	0.458	1.69	0.10	0.86	0.36	0.72	**B-7**	0.755	0.766	0.755	3.52	0.53	3.78	0.48	1.03
A-8	0.410	0.493	0.474	1.76	0.11	1.02	0.33	0.75	**B-8**	0.767	0.791	0.767	1.69	0.62	3.32	0.33	1.15
A-9	0.430	0.509	0.473	1.84	0.12	1.08	0.34	0.77	**B-9**	0.820	0.844	0.820	1.91	0.90	4.50	0.45	1.16
A-10	0.840	0.871	0.861	11.04	0.84	9.26	1.26	0.91	**B-10**	0.753	0.773	0.753	1.64	0.56	2.85	0.34	1.12

A-11	0.890	0.883	0.905	16.79	1.09	14.34	1.67	0.90	**B-11**	0.731	0.751	0.731	1.63	0.49	2.68	0.30	1.12
A-12	0.950	0.922	0.927	25.95	1.33	19.70	3.01	0.81	**B-12**	0.782	0.801	0.782	1.43	0.69	3.28	0.36	1.15
A-13	0.570	0.623	0.605	2.73	0.25	2.14	0.39	0.90	**B-13**	0.554	0.553	0.554	1.39	0.17	1.20	0.22	0.95
A-14	0.570	0.648	0.618	3.73	0.27	2.75	0.52	0.85	**B-14**	0.581	0.562	0.581	1.64	0.20	1.30	0.28	0.92
A-15	0.550	0.643	0.596	4.40	0.25	3.22	0.56	0.81	**B-15**	0.569	0.565	0.569	1.44	0.19	1.31	0.22	0.97
A-16	0.350	0.431	0.397	1.19	0.07	0.67	0.23	0.75	**B-16**	0.513	0.483	0.513	1.04	0.13	0.57	0.25	0.85
A-17	0.380	0.481	0.431	1.49	0.10	0.81	0.30	0.74	**B-17**	0.551	0.534	0.551	1.00	0.17	0.73	0.23	0.93
A-18	0.490	0.557	0.521	1.86	0.17	1.08	0.38	0.81	**B-18**	0.598	0.592	0.598	1.23	0.23	1.08	0.26	0.97
A-19	0.930	0.921	0.917	16.45	1.37	13.61	2.04	0.91	**B-19**	0.501	0.433	0.501	0.75	0.12	0.39	0.21	0.87
A-20	0.990	0.950	0.950	32.15	1.88	21.63	4.81	0.78	**B-20**	0.519	0.508	0.519	0.57	0.14	0.39	0.18	0.94
A-21	1.000	1.000	0.987	75.05	3.36	33.84	17.90	0.62	**B-21**	0.557	0.520	0.557	0.64	0.18	0.55	0.20	0.98
A-22	0.720	0.776	0.764	6.13	0.52	4.68	0.87	0.88	**B-22**	0.474	0.397	0.474	0.69	0.10	0.19	0.24	0.81
A-23	0.770	0.791	0.796	8.02	0.60	6.37	1.00	0.88	**B-23**	0.478	0.453	0.478	0.43	0.10	0.18	0.16	0.89
A-24	0.830	0.822	0.842	9.87	0.73	9.13	0.90	0.95	**B-24**	0.518	0.467	0.518	0.41	0.14	0.27	0.17	0.95
A-25	0.520	0.565	0.551	2.08	0.18	1.60	0.30	0.88									
A-26	0.580	0.607	0.552	2.64	0.23	2.14	0.35	0.90									
A-27	0.600	0.650	0.627	3.54	0.28	2.73	0.48	0.87									

Abbreviations used in the table:

M = measured flow resistance ratio λ_Q.
F-3D (B) = flow resistance ratio obtained with the Flow3D CFD model, using the Bingham material model.
F-3D (HB) = flow resistance ratio obtained with the Flow3D CFD model, using H-B material model.

4.1. Bingham material model vs. H-B material model

The objective of this study is, as mentioned in the introduction, to evaluate whether the flow resistance ratio can be used as a single parameter to describe the flowability of cement paste. However, in order to get to this point, it is necessary to quantify the error that is introduced by going from a three-parameter model (the H-B material model) to a two-parameter model (the Bingham material model). The quantification of this error is carried out by the numerical model. In Figure 5, the difference between the experimental flow resistance ratio and the two numerical predictions are presented. The plot illustrates that for either of the two numerical predictions, the difference does not exceed 30 % in the λ_Q range of 0.3 to 1.0, and the agreement improves when increasing the flow resistance ratio. As reported in [34], a typical range of measurable λ_Q for cements pastes will vary between 0.30-0.75, which also corresponds well to the range of values measured for the pastes studied in the paper. The improvement in the observed difference between the measured and predicted values might be a consequence of the no-slip boundary condition and/or the rheological approximation functions favouring a slow flow. Furthermore, Figure 5 demonstrates that generally the best agreement is obtained, when using the H-B material model in the numerical simulations. The average difference in absolute values for the Bingham and H-B material model is 6.5 and 4.6 %, respectively, thus illustrating that an additional error of approx. 2 % can be expected when assuming the two-parameter material model instead of the three-parameter material model. This error is specific for the flow condition in the FlowCyl where the shear rates can vary in the order of 0 – 290 1/s, see Figure 6 that presents simulation results for mix No. A-6. Note that these shear rates are experienced at a height of 25 cm, which is in the middle of the measuring interval, and that greater shear rates are experienced at the start of the measuring interval (35 cm), as the hydrostatic head is larger. Within the shear rate interval 0 – 290 1/s, the two material models approximate the measured rheological data as seen in Figure 7 for mix No. A-6. The rheometer experiments are carried out up until a shear rate of 60 1/s, whereas the shear rates in the FlowCyl are greater, as predicted by the numerical simulations, see Figure 6. This is a source of error that leads to a difference between the experimental and numerical flow resistance ratio. In addition, there could also be a potential error associated with how good the models are able to approximate the actual rheological response of the materials, which was found to be more precise in the case of the H-B model, see Figure 6. Figure 7 shows that at shear rates above 60 1/s, the material models start to deviate from each other, which is the main reason for the difference in the predicted flow resistance ratios between the two models shown in Figure 5. The shear rate interval experienced by the cement paste during concrete mixing and placement is in the order 0–70 1/s [35]. This upper shear rate limit is less than the one experienced in the FlowCyl, which indicates that modifying the flowrate in the FlowCyl to lower the shear rate is relevant.

4.2. Effect of the rheological properties on the measured flow resistance ratio

Knowing that the error that is introduced going from the H-B- to the Bingham material model is relatively sparse (see previous section), the rest of the analysis focus on going from a two-parameter (the Bingham material model) to a one-parameter (the flow resistance ratio) flow characterization. In Figure 8 and Figure 9, the experimental flow resistance ratio is plotted as function of the plastic viscosity and yield stress, respectively. In the figures, additional 42 results from a previous study [16] are included in order to cover a broader rheological interval. The mixes in [16] were carried out with ten different types of fillers, fi/c ratios by volume ranging from 0.4 to 0.5, a w/c ratio of 0.5, and constant SP dosage of 0.50 % per mass cement. Figure 8 shows that all the measurements collapse on the same curve in the flow resistance ratio vs. plastic viscosity plot, whereas Figure 9 shows that the same trend is not the case for the flow resistance ratio vs. yield stress plot. This illustrates that the plastic viscosity dominates the flow resistance ratio, a finding that theoretically was predicted by the numerical model as seen in [13]. This can be illustrated by the following example where the apparent viscosity is calculated for mix No. A-6 at the outlet as well as for two hypothetical cement pastes; one where the yield stress is increased with 50 % and another where the plastic viscosity is increased with 50 %, both as compared to mix No. A-6. The three cement pastes have the following rheological properties: 1) τ_0 = 4.85 Pa and μ = 0.38 Pas; 2) τ_0 = 7.28 Pa and μ = 0.38 Pas; and 3) τ_0 = 4.85 Pa and μ = 0.57 Pas. The apparent viscosity is calculated for the three cement pastes at a representative shear rate of 150 s^{-1}. This value is obtained by considering the shear rates at a height of 25 cm (*i.e.* the middle of the measuring interval) and then taking the average shear rate over the cross section in the bottom of the FlowCyl.

$\mu_{app,1} = \tau/\dot{\gamma} = \tau_0/\dot{\gamma} + \mu = 4.85/150 + 0.38 = 0.412$ Pas;

$\mu_{app,2} = \tau/\dot{\gamma} = \tau_0/\dot{\gamma} + \mu = 7.28/150 + 0.38 = 0.429$ Pas;

$\mu_{app,3} = \tau/\dot{\gamma} = \tau_0/\dot{\gamma} + \mu = 4.85/150 + 0.57 = 0.602$ Pas.

The above examples show that a 50 % increase in the yield stress (from 4.85 Pa to 7.28 Pa) only makes the apparent viscosity increase by approx. 4 %, whereas a 50 % increase in the plastic viscosity (from 0.38 Pas to 0.57 Pas) makes the apparent viscosity increase by approx. 50 %. This example explains why the flow resistance ratio primarily depends on the plastic viscosity of the materials in the FlowCyl. The reason for the dominance is owed to the fact that the cement paste experiences high shear rates at the outlet, see Figure 6, which is a region of the FlowCyl that has a great influence on the flow rate and thereby the flow resistance ratio. These high shear rates lead to apparent viscosities (the viscosity felt by the flowing cement paste) that are dominated by the plastic viscosity in the Bingham material model. As a result, one can state that the flow resistance ratio can be used as a one-parameter characterization of cement paste rheology, as long as the shear rates that the cement paste undergoes in the given application are high. However, this statement only covers a part of the usefulness/limitations of the flow resistance ratio. This is because it is generally accepted that the SP is mainly affecting the yield stress [36], whereas the plastic viscosity is mainly affected by the solid fraction [37]. Therefore, we conducted the “B”-series in this study. Figure 10 shows the plastic viscosity vs. yield stress of the B-series. It illustrates that the SP dosage per cement mass primarily affects the yield stress, as expected, and thereby the slope of the linear relationship between the plastic viscosity and yield stress. Consequently, one single curve cannot represent the flow resistance ratio vs. yield stress measurements, because the flow resistance ratio does not capture the effect of the change in the yield stress. Hence, the SP-dosage per cement mass affects the usefulness of the flow resistance ratio as a one parameter characterization. Further research should therefore look for ways to make the flow resistance ratio more sensitive to the yield stress, *e.g.* by lowering the rate of shear in the FlowCyl.

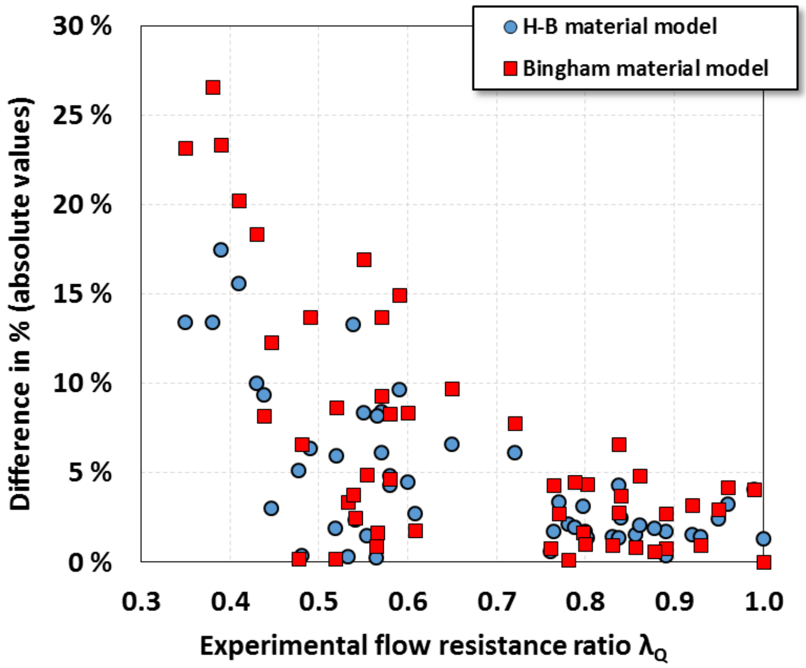

Figure 5: The difference in percentage between the experimental and numerical flow resistance ratio obtained with both the Bingham- and H-B material model. The difference is presented in absolute values. The average difference for the Bingham material model is 6.5 %, while it is 4.6 % for the H-B material model.

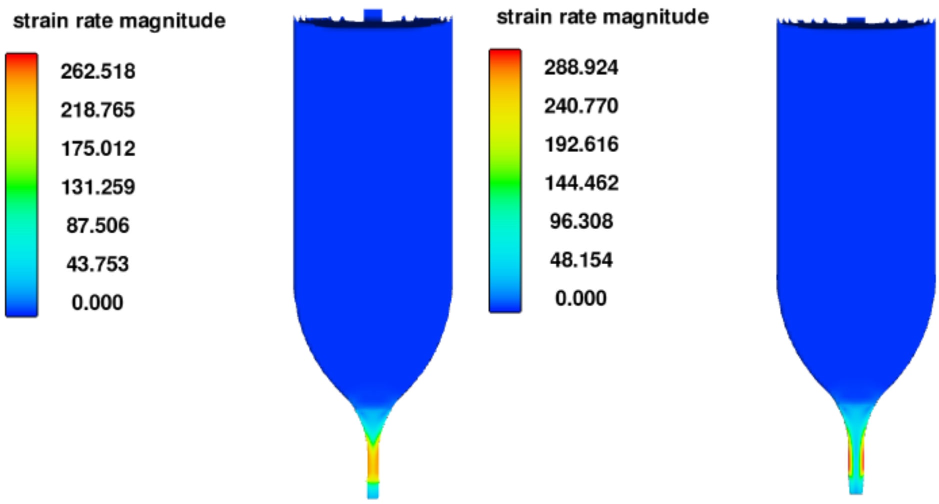

Figure 6: The shear rate magnitude in the cross section of the FlowCyl for mix No. A-6 at a height of 25 cm: left) Bingham material model right) H-B model. Note that the strain rates are in 1/s.

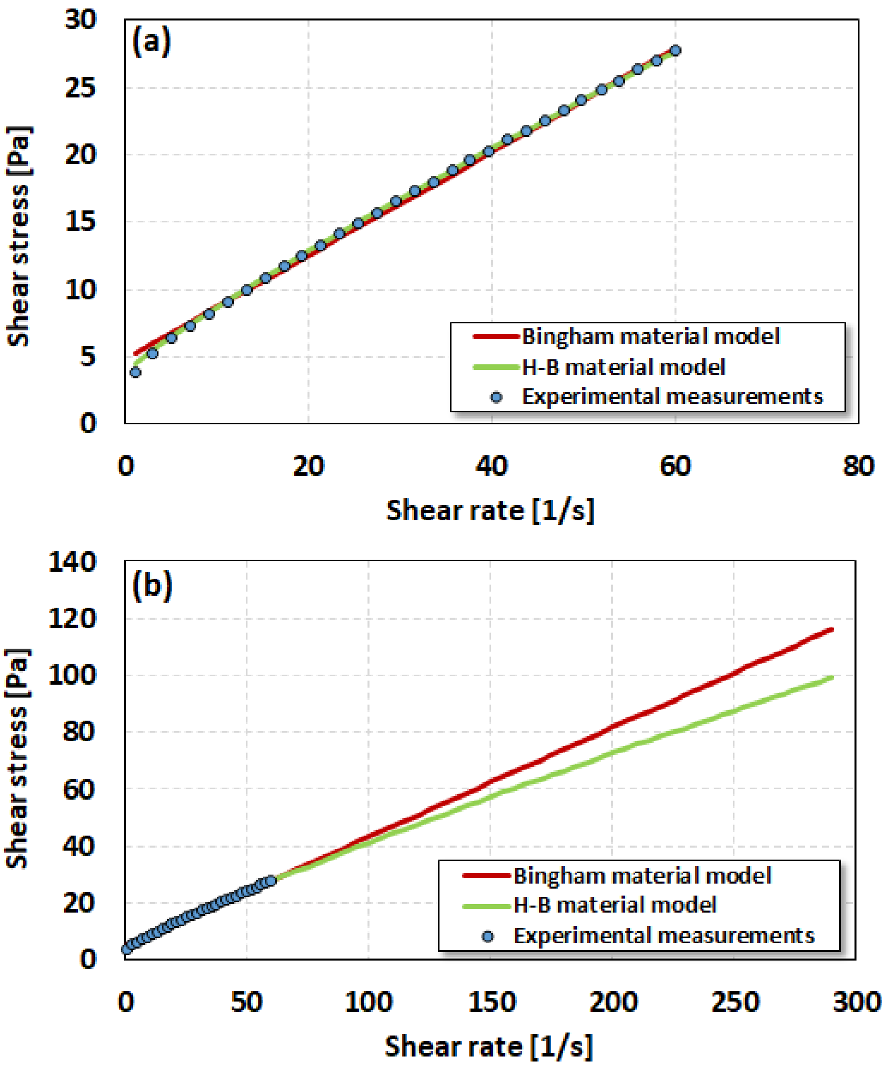

Figure 7: The rheological measurements for mix No. A-6 together with the fits based on the Bingham and H-B model: a) plotted until a shear rate of 60 1/s, b) plotted until a shear rate of 290 1/s.

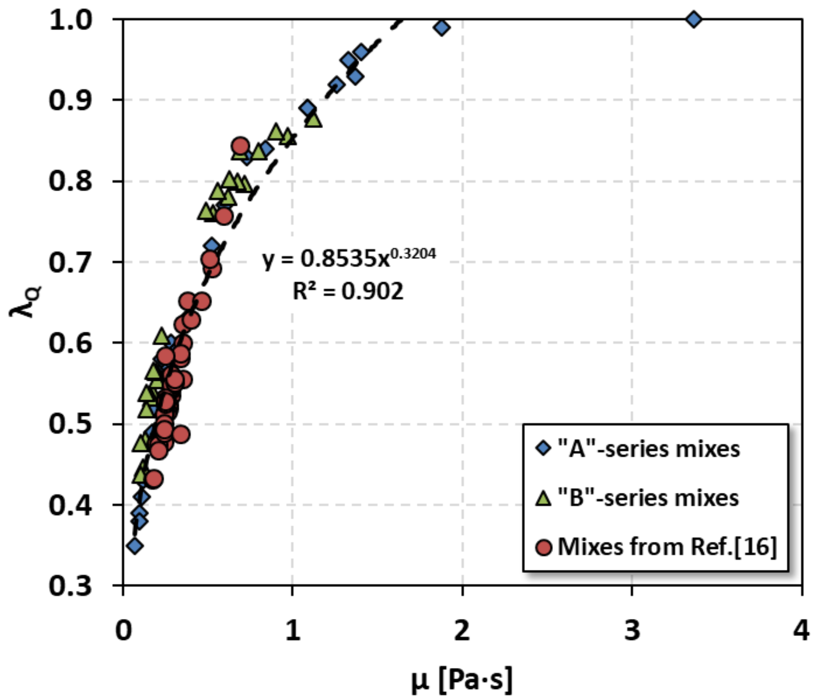

Figure 8: Flow resistance ratio vs. plastic viscosity for all the experiments and mixes from Ref. [16]. Note that the experimental point corresponding to λ_Q=1 represents a cement paste matrix that was not flowing in the FlowCyl equipment, and this it is in fact its rheological parameters are outside the measurement range of the equipment.

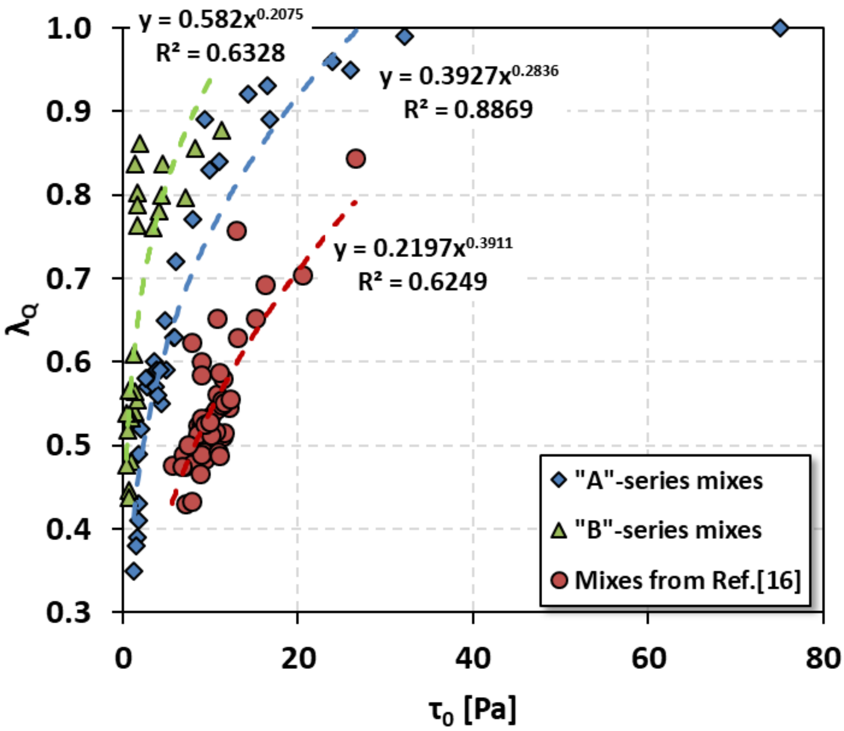

Figure 9: Flow resistance ratio vs. Bingham's yield stress for all the experiments and mixes from Ref. [16]. Note that the experimental point corresponding to λ_Q=1 represents a cement paste matrix that was not flowing in the

FlowCyl equipment, and this it is in fact its rheological parameters are outside the measurement range of the equipment.

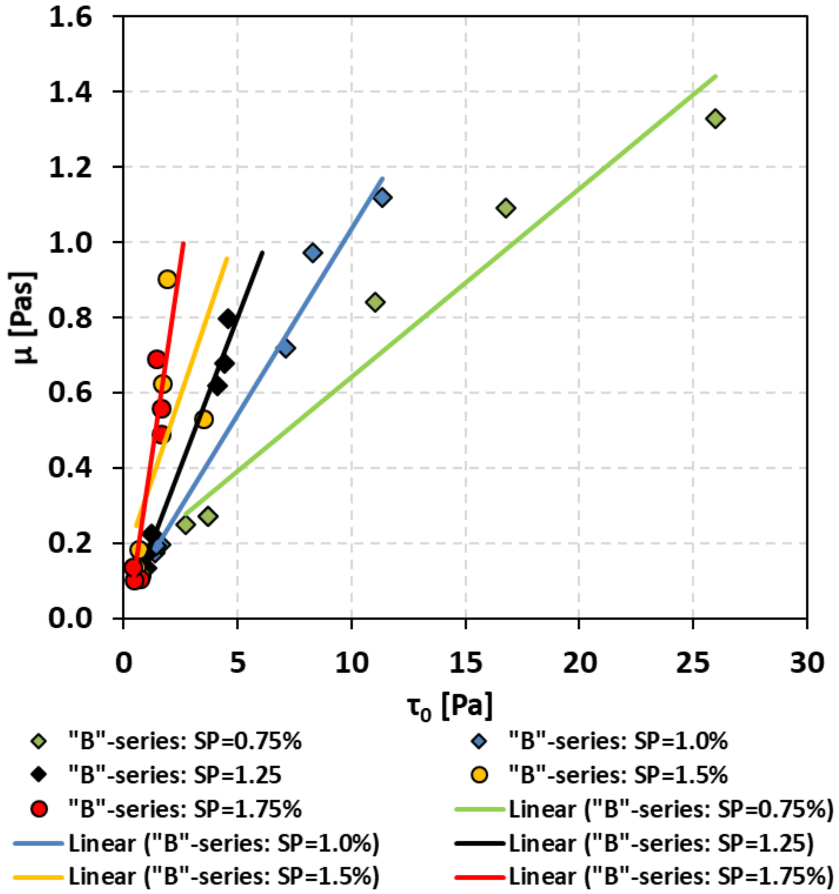

Figure 10: Plastic viscosity vs. yield stress for "B"-series mixes where the SP dosage per cement mass was varied.

5. CONCLUSIONS

For the cement pastes investigated experimentally and numerically in this study, the following main conclusions can be drawn with respect to the limitations of the FlowCyl and appertaining flow resistance ratio:

- The average difference between the experimental and numerical flow resistance ratio is 6.5 % and 4.6 % with the Bingham and H-B material model, respectively. Thus, indicating that an additional error of approx. 2 % can be expected when assuming that the cement paste can be described with the two-parameter material model (Bingham material model) instead of the three-parameter material model (H-B material model);

- All the measurements collapse on the same curve in the flow resistance ratio vs. plastic viscosity plot, which is not the case for the flow resistance ratio vs. yield stress plot. This illustrates that the flow resistance ratio is dominated by the plastic viscosity. This finding is supported by the numerical model that predicts very high shear rates at the outlet. As a consequence, it is argued that the flow resistance ratio can be used as a one-parameter characterization of cement paste rheology, when the shear rates that the cement paste undergoes in a given application are high;
- The SP dosage per mass cement changes the slope of the apparent linear relationship between the yield stress and plastic viscosity. For that reason, it is also argued that the flow resistance ratio can distinguish between the flowability of cement pastes if the SP dosage per mass cement is kept constant;
- Further work will be targeted at changing the FlowCyl design to decrease the shear rate at the outlet and thereby enable the one-parameter flow resistance ratio to become sensitive to variations in the yield stress.

ACKNOWLEDGEMENTS

The study presented in this paper is performed within the MiKS project – Mikroproporsjonering med Knust Sand (Norwegian for Micro-proportioning with Crushed Sand), which is a KPN (Competence Project for the Industry) funded by the Research Council of Norway (RCN) contract No. 247619 and industrial partners. The authors would like to thank the RCN and the industrial partners (Norcem AS, Skanska Norge AS and Feiring Bruk AS) for their financial contribution to the research.

REFERENCES

[1] C. Ferraris, K. Obla and R. Hill, “The influence of mineral admixtures on the rheology of cement paste and concrete,” *Cement and Concrete Research,* vol. 31, no. 2, pp. 245-255, 2001.

[2] E. Mørtsell, “Modelling the effect of concrete part materials on concrete consistency. PhD,” Norwegian University of Science and Technology (In Norwegian), 1996.

[3] S. Smeplass, “BE96-3942/R12 Applicability of the particle-matrix model to LWAC,” EuroLightCon, Brussels, 2000.

[4] J. Wallevik, “Rheological properties of cement paste: Thixotropic behaviour and structural breakdown,” *Cement and Concrete Research,* vol. 39, pp. 14-29, 2009.

[5] T. Mezger, The Rheology Handbook: For users of rotational and oscillatory rheometers, Hannover: Vincentz Network, 2006.

[6] R. Shaughnessy and P. Clark, “The rheological behaviour of fresh,” *Cement and Concrete Research,* vol. 18, pp. 327-341, 1988.

[7] D. Feys, R. Cepuritis, S. Jacobsen, K. Lesage, E. Secrieru and A. Yahia, “Measuring rheological properties of cement pastes: most common techniques, procedures and challenges,” *RILEM Technical Letters,* vol. 2, pp. 129-135, 2017.

[8] N. Roussel, C. Stefani and R. Leroy, “From mini-cone test to Abrams cone test: measurement of cement-based materials yield stress using slump tests,” *Cement and Concrete Research,* vol. 35, pp. 817-822, 2005.

[9] N. Roussel and R. Le Roy, “The Marsh cone: a test or a rheological appartus?,” *Cement and Concrete Research,* vol. 35, pp. 823-830, 2005.

[10] R. Le Roy and N. Roussel, “The Marsh Cone as a viscometer: theoretical analysis and practical limits,” *Materials and Structures,* vol. 38, no. January-February, pp. 25-30, 2005.

[11] S. Smeplass and E. Mørtsell, “The applicability of the particle matrix model to self compacting concrete,” *Nordic Concrete Research,* vol. 26, 2001.

[12] T. Hammer and J. Wallevik, “On the correlation between rheology of paste, mortar and concrete,” in *Proceedings of the Second North American Conference on the Design and Use of Self-Consolidating Concrete (SCC) and the Fourth International RILEM Symposium on Self-Compacting Concrete*, Chicago, 2005.

[13] R. Cepuritis, E. Ramenskiy, E. Mørtsell, S. Smeplass, H. Kjos-Hanssen, S. Li, S. Jacobsen and J. Spangenberg, “FlowCyl: one-parameter characterisation of matrix rheology,” in *Proceedings of the Second Concrete Innovation Conference (2nd CIC), 6-8 March,* Tromsø, Norway, 2017.

[14] H. Merkus, Particle Size Measurements. Fundamentals, Practice, Quality, Dordrecht: Springer Science+Business Media B.V., 2009.

[15] S. Ng., H. Mujica and S. Smeplass, “Design of a simple and cost-efficient mixer for matrix rheology testing,” *Nordic Concrete Research,* vol. 51, no. 3, pp. 15-28, 2014.

[16] R. Cepuritis, "Development of Crushed Sand for Concrete Production with Micro-proportioning. PhD," Norwegian University of Science and Technology, Trondheim, 2016.

[17] R. Cepuritis, S. Jacobsen, S. Smeplass, E. Mørtsell, B. Wigum and S. Ng, "Influence of crushed aggregate fines with micro-proportioned particle size distributions on rheology of cement paste," *Cement and Concrete Composites,* vol. 80, pp. 64-79, 2017.

[18] K. Vasilic, W. Schmidt, H. Kühne, F. Haamkens, V. Mechtcherine and N. Roussel, "Flow of fresh concrete through reinforced elements: Experimental validation of the porous analogy numerical method," *Cement and Concrete Research,* vol. 88, pp. 1-6, 2016.

[19] K. Vasilic, B. Meng, H. Kühne and N. Roussel, "Flow of fresh concrete through steel bars: A porous medium analogy," *Cement and Concrete Research,* vol. 41, pp. 496-503, 2011.

[20] S. Jacobsen, R. Cepuritis, Y. Peng, M. Geiker and J. Spangenberg, "Visualizing and simulating flow conditions in concrete form filling using pigments," *Construction and Building Materials,* vol. 49, pp. 328-342, 2013.

[21] L. Shen, L. Struble and D. Lange, "Modelling dynamic segregation of self-consolidation concrete," *ACI Mater. J.,* pp. 375-380, 2009.

[22] J. Spangenberg, N. Roussel, J. Hattel, H. Stang, J. Skocek and M. Geiker, "Flow induced particle migration in fresh concrete: Theoretical frame, numerical simulations and experimental results on model fluids," *Cement and Concrete Research,* pp. 633-641, 2012.

[23] J. Spangenberg, N. Roussel, J. Hattel, E. Sarmiento, G. Zirgulis and M. Geiker, "Patterns of gravity induced aggregate migration during casting of fluid concretes," *Cement and Concrete Research,* pp. 1571-1578, 2012.

[24] J. Wallevik, W. Mansour and O. Wallevik, "OpenFOAM casting solver with segregation. International RILEM conference on materials, systems and Structures in Civil Engineering, Conference segment on Fresh Concrete," in *Published by RILEM Publications S.A.R.L. ISBN: 978-2-35158-184-1,* 22-24 August, Technical University of Denmark, Lyngby, Denmark, 2016.

[25] O. Svec, G. Zirgulis, J. Bolander and H. Stang, "Influence of formwork surface on the orientation of steel fibres within self-compacting concrete and on the mechanical

properties of cast structural elements," *Cement & Concrete Composites,* vol. 50, pp. 60-72, 2014.

[26] L. Martinie, J.-F. Lataste and N. Roussel, "Fiber orientation during casting of UHPFRC: electrical resistivity measurements, image analysis and numerical simulations," *Materials and Structures,* vol. 48, pp. 947 - 957, 2015.

[27] H. Le, E. Kadri, S. Aggoun, J. Vierendeels, P. Troch and G. De Schutter, "Effect of lubrication layer on velocity profile of concrete in a pumping pipe," *Mater. Struct.*, vol. 48, pp. 3991-4003, 2008.

[28] J. Wallevik, "Minimizing end-effects in the coaxial cylinders viscometer: Viscoplastic flow inside the ConTec BML Viscometer 3," *J. Non-Newtonian Fluid Mech.,* pp. 116-123, 2008.

[29] A. Gram, J. Silfwerbrand and B. Lagerblad, "Obtaining rheological parameters from flow test — Analytical, computational and lab test approach," *Cement and Concrete Research,* vol. 63, pp. 29-34, 2014.

[30] N. Roussel, A. Gram, M. Cremonesi, L. K. K. Ferrara, V. Mechtcherine, S. Shyshko, J. Skocek, J. Spangenberg, O. Svec, L. Thrane and K. Vasilic, "Numerical simulations of concrete flow: A benchmark comparision," *Cement and Concrete Research,* vol. 79, pp. 265-271, 2016.

[31] C. Hirt and B. Nichols, "Volume of fluid (VOF) method for the dynamics of free boundaries," *J. Comput. Phys.,* pp. 201-225, 1981.

[32] R. Comminal, J. Spangenberg and J. Hattel, "Cellwise conservative unsplit advection for the volume of fluid method," *J. Comput. Phys.,* pp. 582-608, 2015.

[33] E. Mitsoulis, "Flows of viscoplastic materials: models and computations," *Rheol. Rev.,* pp. 135-178, 2007.

[34] S. Smeplass and R. Cepuritis, "Chapter 4 - Fresh concrete - proportioning," in *TKT 4215 Concrete Technology 1, course compendium*, Trondheim, Norwegian University of Science and Technology, 2016, pp. 4.1-4.41.

[35] R. Helmuth, L. Hills, D. Whitting and S. Bhattacharja, "Abnormal Concrete Performance in the Presence of Admixtures. PCA R&D Serial No. 2006," Portland Cement Association, Skokie, 2006.

[36] O. Wallevik and J. Wallevik, “Rheology as a tool in concrete science: The use of rheographs and workability boxes,” *Cement and Concrete Research,* vol. 41, no. 12, pp. 1279-1288, 2011.

[37] H. Barnes, J. Hutton and K. Walters, Introduction to Rheology, Amsterdam: Elsevier Science Publishers B.V., 1993.